X-514-67-447

NASA TM X-55950

INTERCOMPARISON OF COLLOCATED LASER OPTICAL AND GRARR RADIO RANGING SYSTEM TRACKS ON GEOS-A

GPO PRICE $ ______

CFSTI PRICE(S) $ ______

Hard copy (HC) 3.00

Microfiche (MF) .65

ff 653 July 65

SEPTEMBER 1967

FACILITY FORM 602

N67-39092 (ACCESSION NUMBER)

(THRU)

38 (PAGES)

1 (CODE)

TMX-55950 (NASA CR OR TMX OR AD NUMBER)

07 (CATEGORY)

NASA

GODDARD SPACE FLIGHT CENTER
GREENBELT, MARYLAND

INTERCOMPARISON OF COLLOCATED LASER OPTICAL AND GRARR RADIO RANGING SYSTEM TRACKS ON GEOS-A

REVIEW AND CONCURRENCE SHEET

Head, Operations Evaluation Branch	John H Berbert John H. Berbert
Chief, Project Operations Support Division	Albert G. Ferris Albert G. Ferris

INTERCOMPARISON OF COLLOCATED LASER OPTICAL AND GRARR RADIO RANGING SYSTEM TRACKS ON GEOS-A

Principal Contributors

John H. Berbert
(NASA) Principal Investigator
GEOS Observation Systems Intercomparison Investigation

Paul Maresca, Patrick Norris,
and Robert Reich
RCA Service Company

September 1967

GODDARD SPACE FLIGHT CENTER
Greenbelt, Maryland

INTERCOMPARISON OF COLLOCATED LASER OPTICAL AND GRARR RADIO RANGING SYSTEM TRACKS ON GEOS-A

Principal Contributors

John H. Berbert
(NASA) Principal Investigator
GEOS Observation Systems Intercomparison Investigation

Paul Maresca, Patrick Norris,
and Robert Reich
RCA Service Company

ABSTRACT

NASA is conducting a Geodetic Earth Orbiting Satellite-A (GEOS-A) Observation Systems Intercomparison Investigation. As part of this investigation, some tests consisted of side-by-side tracking of the GEOS-A spacecraft by the Goddard Range and Range Rate (GRARR) system and the Goddard Laser tracking system. Seventeen passes were observed from July to November 1966 by the Rosman, North Carolina GRARR station and 10 of these were evaluated. In the investigation, the Laser system tracks of the spacecraft were used as a reference trajectory for the GRARR system. The Laser data was smoothed using the GEOS-A Data Adjustment Program (GDAP) giving a reference orbit at the selected time of epoch in the form of a cartesian position and velocity vector. The evaluation of data shows that Laser orbits can be used to detect systematic errors in both range and range rate to about 2 meters and 1 centimeter per second respectively.

Using the measured GRARR data and Laser orbital elements, GDAP determined the average range zero-set bias error to be -5.3 meters with a standard deviation of ± 2.5 meters per pass for seven of the ten passes. The other three passes were outliers with biases up to 30 meters from the established average. The range-timing error was determined to be -2.1 ± 1.2 milliseconds. The unsmoothed range data RMS noise component was 6.8 meters after systematic errors were removed. It is assumed that inaccuracies in the transponder delay curve resulted in GRARR range-bias and timing errors.

The range-rate residuals from GDAP were corrected for refraction and a sequential least squares regression program used to estimate coefficients in various range-rate error models. No significant range-rate zero-set bias was detected. A consistent range-rate timing error of $-0.20 \pm .02$ milliseconds was observed, but its cause was not detected. A frequency-scale-factor error of about 10 parts per million was also observed. The unsmoothed range-rate data RMS component was 1 centimeter per second after these systematic errors were removed.

TABLE OF CONTENTS

LIST OF ILLUSTRATIONS

LIST OF TABLES

TABLE OF CONTENTS (Cont)

INTRODUCTION

As part of the Geodetic Earth Orbiting Satellite-A (GEOS-A) Observation Systems Intercomparison Investigation, several groups of tests were conducted from July 1966 through November 1966 at Rosman, North Carolina. These tests consisted of side-by-side tracking of the GEOS-A spacecraft by the Goddard Range and Range Rate (GRARR) system and the Goddard Laser tracking system. The tests were conducted to aid in the evaluation of the GRARR system and to determine the effectiveness of the Laser as a calibration instrument for electronic tracking systems. A list of the spacecraft passes and a brief description of the data taken are given in Table 1.

Table 1
Spacecraft Passes

Run No.	Date	Remarks
1 2	July 27 July 28	The Laser was in a multipulse mode of operation. In this mode more than one pulse is issued in the normal excitation period of one second making the data unusable in its present form. It may be possible to recover this type of data by separating it into pulse subsets and applying the smoothing techniques to each subset.
3	July 29	No tracking overlap occurred between the GRARR system and the Laser system.
4	August 10	The Laser system suffered a timing synchronization problem in which the Laser time was from zero to three milliseconds in error. This effectively increased the Laser RMS error from 2 to 4 meters. Also, the span of overlap tracking was short.
5	Sept. 9	The GRARR system reported a rate aid tracking problem; hence the error in the data is quite large. Also, an ambiguity transition of approximately 7500 meters occurred during the pass. When each section (before and after transition) was analyzed separately, a significant difference in GRARR bias was present. However, no timing

Table 1
Spacecraft Passes (Cont)

Run No.	Date	Remarks
		anomaly was incorporated in the above analysis. For this type of data, if the two subgroups are combined after an ambiguity correction and a time correction are applied, the data may be useful.
6	Sept. 10	This pass was not useful because of an unusual drift in the GRARR data.
7	Oct. 5	No GRARR data was taken.
8 9 10	Oct. 6 Oct. 7 Oct. 8	The Laser data suffered from a dropped bit equivalent to thirty meters when certain data word configurations were encountered. This fault was quickly isolated to a gate malfunction in the range counter. The dropped bits were isolated by first smoothing all data, recognizing and deleting the erroneous data points, and resmoothing the remaining data.
11	Nov. 15	This pass was quite short and tracking did not begin until after the point of zero range rate; hence, results were inconclusive.
12	Nov. 18	This pass showed an unusually large GRARR range bias.
13	Nov. 19	This proved a good pass, but relatively short.
14	Nov. 19	There was no overlap between the systems.
15	Nov. 20	This was a good pass.
16	Nov. 20	This was a good pass but had a larger than normal GRARR range bias.
17	Nov. 21	This was a good pass.

The Laser system tracks of GEOS-A were used as a reference trajectory for the GRARR system. The Laser data was smoothed using the GEOS-A Data Adjustment

Program (GDAP)[1] giving a reference orbit at the selected time of epoch in the form of a cartesian position and velocity vector. Then using the measured GRARR data and the Laser orbital elements, GDAP determined the range zero set error and the timing error for each pass. The range rate residuals from GDAP were corrected for refraction and a sequential least squares regression program[2, 3] used to estimate coefficients in various range and range rate error models. The results were analyzed to determine the appropriate models.

LASER SYSTEM

The Laser tracking system placed at Rosman for these tests uses an intense, highly-collimated, short-duration beam of light for illuminating the spacecraft being tracked. The beam is reflected at the spacecraft by special reflecting surfaces and the returning light is detected photoelectrically, and its time of flight measured to yield range data. The actual laser transmitter was mounted on a radar pedestal along with a Cassegrainian telescope used for receiving the reflected Laser beam. When the Laser system is tracking, the transmitter is flashed at one pulse per second. Each transmitted pulse starts a time interval measuring unit necessary for range measurement. During the pass, the mount equipped with digital encoders, is directed toward the expected position of the spacecraft by a programmer fed with punched paper tape. By using a telescope, the operator can see the spacecraft and make corrections to keep it within the illuminating beam. Along with a range measurement, both the azimuth and elevation of the spacecraft are recorded from the position of the mount. These angles are used for parallax corrections on the GDAP but not in the actual orbit determination since they need be accurate enough only for acquisition of the spacecraft and the driving of the mount during tracking.

LASER SYSTEM PREPROCESSING

The Laser tracking data consists of one measurement per second of range in nanoseconds and elevation and azimuth in degrees punched on paper tape. Using an AD/ECS-37 computer, punched cards are produced from the tape. Using a preprocessing program, the following corrections are added to the whole-second time for each measurement to give the time at the spacecraft.

- WWV correction (3.6 milliseconds for Rosman).
- Delay time between the on-second pulse and actual Laser firing.
- One-half the round trip interval of the Laser beam.

The following correction is made to each range measurement when it is converted from a time interval into meters:

- Internal delay correction due to photomultiplier, cables and receiving telescope (90 nanoseconds round trip).

The corrected range, azimuth, and elevation measurements are put into a format acceptable to GDAP.

GRARR SYSTEM

The GRARR system is a high-precision, spacecraft-tracking system that determines range using the sidetone ranging technique, and range rate applying the principles of coherent doppler. Angular data is obtained from X-Y mounted antennas but is not used for orbit determination. Each GRARR station uses an S-band system and a VHF system[4] in conjunction with a multichannel transponder on the spacecraft being tracked. Only the S-band system was used for this evaluation. The *a-priori* estimates of random errors are presented in Tables 2 and 3.

GRARR SYSTEM PREPROCESSING

Data at one measurement per second consisting of the range in meters, range rate in meters per second, and X and Y angles in degrees were used for this evaluation. In the operational preprocessing, the times are corrected to the spacecraft and a constant transponder bias correction equivalent to 3677 nanoseconds is made for each range measurement before submission to the Data Center at Goddard. For this evaluation the following corrections are made to each range measurement (R_m) in addition to the usual operational preprocessing described above:

It should be noted that Table 2 is the same as Table 4 in the Goddard document "Evaluation of Range Accuracy for the GRARR System at Rosman".[6] However, the random range error due to transponder group delay variations has been omitted since this error is now modeled by the transponder delay curve used in the GRARR preprocessing.

Table 2
GRARR Range Estimated Random Errors[5]

Name	High Frequency (in meters)	Low Frequency (in meters)
Oscillator noise	0.2	0.0
Thermal noise	0.7	0.0
Quantization	0.6	0.0
Digital timing	4.5	2.8
Receiver delay variations	0.0	2.0
Oscillator calibrations	0.0	0.5
Transponder temperature and S/N variation delays	0.7	0.7
Sub-total (RMS)	4.7	3.5
Combined total (RMS)	5.8	

Table 3
GRARR Range Rate Estimated Random Errors

Name	Random Errors (cm/sec)
Thermal noise	0.1
Coherent oscillator instability	0.1
Oscillator noise	1.0
Quantizing noise	0.5
Coherent oscillator calibration	0.0
Digital timing errors	0.4
Total (RMS)	1.2

- Additional uncorrected ground station system delays (Rosman, N.C.)

$$\Delta R_1 = 9.7 \text{ meters}$$

- Transponder delay (Channel A)

$$\Delta R_2 = (7.18 \times 10^{-8}) \dot{R}^2 + (3.32 \times 10^{-4}) \dot{R} \text{ meters}$$

- Axis offset correction

$$\Delta R_3 = 1.17 \cos Y \text{ meters}$$

The final range (R_T) used is calculated by:

$$R_T = R_M + \Delta R_1 - \Delta R_2 + \Delta R_3 \text{ meters}$$

No additional preprocessing corrections are made to the range rate data.

There are two deterministic corrections which were not applied to the GRARR data at the time of processing. The first is the pre- and post-calibration adjustments which are now available. It is believed that these could affect some of the bias values by approximately one meter. The second is the WWV time synchronization information. Because of the direct time link between the systems, this would not have affected the intercomparison results.

GEOS DATA ADJUSTMENT PROGRAM (GDAP)

After preprocessing has been completed, the GDAP determines a simultaneous solution to all the observation equations, which minimizes the weighted sum of squares of the residuals between these equations and the actual observations. Thus at any time T_j we minimize:

$$F_j = \sum_i \left[w_i f_i (X_j, Y_j, Z_j, \dot{X}_j, \dot{Y}_j, \dot{Z}_j, T_j, p_1, \ldots p_n) \right]^2$$

where $f_i = D_i$, observed $- D_i$, corrected. The sum is taken over all data points. D_i indicates the measurement, range, range rate or other data being processed. X_j, Y_j, . . . etc. are the orbital parameters for position and velocity, $T_j = t_j - t_o$ where t_o is an epoch time, $p_1, \ldots p_n$ are error model parameters such as station location, zero set bias, etc., and w_i is a weight based on a-priori standard error inputs.

The implementation of the solution of the simultaneous equations depends upon the linearization of the equation set by expansion in a Taylor's series about a given approximation to the solutions. The resulting set of linear simultaneous equations is commonly known as the set of normal equations, and in matrix form is given by:

$$N\delta = C$$

where:

$$N = B^T W B$$

and:

$$C = B^T W E$$

The matrix B is called the matrizant and is the matrix of partial derivatives of the parameters at time t_j with respect to the parameters at the time of epoch, t_o, and for the orbital parameters is represented by:

$$B = \begin{bmatrix} \frac{\partial X_j}{X_o} & \cdots\cdots & \frac{\partial X_j}{\dot{Z}_o} \\ \vdots & & \vdots \\ \frac{\partial \dot{Z}_j}{X_o} & \cdots\cdots & \frac{\partial \dot{Z}_j}{\dot{Z}_o} \end{bmatrix}$$

The matrix W is the weighting matrix and is the inverse of the covariance matrix which is initially formed using a-priori input standard deviations of the parameters. The vector E is given by:

$$\begin{bmatrix} X_j\text{, observed } - X_j\text{, corrected} \\ \vdots \\ \dot{Z}_j\text{, observed } - \dot{Z}_j\text{, corrected} \end{bmatrix}$$

The normal equations are solved for the vector of parametric corrections, δ using matrix inversion. The solution, thus produced, is used to update or correct the current approximations to the error model coefficients. The solution is then iterated until the corrections are all equal to or less than one-half the a-posteriori standard error estimates, at which time the solution is complete. If the normal equations are properly formulated, they yield as a by-product of the calculation, the inverse normal equation coefficient matrix which is given by:

$$V_j = \begin{bmatrix} \sigma X_j^2 & \sigma X_j, Y_j & \ldots & \sigma X_j, Z_j \\ \sigma Y_j, X_j & \sigma Y_j^2 & \ldots & \sigma Y_j, \dot{Z}_j \\ \vdots & \vdots & & \vdots \\ \sigma \dot{Z}_j, X_j & \sigma \dot{Z}_j, Y_j & \ldots & \sigma \dot{Z}_j^2 \end{bmatrix}$$

This matrix has the property of being the covariance matrix of the parameter correction values. This covariance matrix provides an indication of the remaining uncertainty in the determined values of the coefficients.

LASER ERROR MODEL

For the Laser passes, the GDAP state variables included the orbital elements described by position and velocity X, Y, Z, $\dot{X}$, $\dot{Y}$, $\dot{Z}$ in cartesian coordinates at epoch time. The initial estimates of these parameters were obtained from Minitrack orbital predictions and were unconstrained. Also, an azimuth bias and an elevation bias were used as state variables with an initial estimate of zero and an a-priori standard error of .5 milliradians for both.

GRARR ERROR MODEL

The orbital elements used for the GRARR passes were the converged values of the orbital elements from the same Laser pass. They were held constant by using a very small a-priori standard deviation. The radar error model included a zero-set bias parameter, initially estimated to be zero but allowed to vary freely by being given a very large a-priori standard deviation. There was also, in the error model a timing error term that was to detect any difference between the Laser and the GRARR range timing. This, too, was initially estimated to be zero since the difference was expected to be no more than one hundred microseconds. Again this parameter was allowed to vary by giving the initial estimate a small weight.

SUMMARY OF RESULTS

Data were obtained from collocated Laser and GRARR systems at Rosman for seventeen passes. Tables 4 and 5 give a summary of the Laser and GRRAR results, respectively. The average bias error for the Rosman GRARR relative to the Laser was found to be -5.3 ± 2.5 meters. The random noise after removal of the bias was 6.8 meters. The average timing difference between the Laser and the GRARR range timing was -2.1 ± 1.2 milliseconds. Later it is shown that the average difference between the Laser and the GRARR range rate timing is only -0.20 ± 0.02 milliseconds.

ANALYSIS OF ERRORS

In order to investigate further the sources of error in the GRARR system, three passes were chosen for closer examination. The passes used were passes 10, 15 and 17. Bias, RMS and range timing errors for these passes can be found in Table 5, while Table 6 gives average values for the three passes above.

Table 4
Summary of Laser Data

Run No.	Date	Pass Duration (seconds)	Range RMS (meters)	Azimuth RMS (milliradians)	Elevation RMS (milliradians)
1	July 27	392	27.1*	.34	1.91
2	July 28	252	17.1*	.17	.11
3	July 29	no overlap	2.1	.20	.15
4	Aug. 10	96	4.3	.14	.09
5	Sept. 9	345	2.1	.27	.16
6	Sept. 10	304	1.5	.20	.07
8	Oct. 6	205	1.7	1.07	.14
9	Oct. 7	377	1.6	1.11	.24
10	Oct. 8	344	1.2	.26	.13
11	Nov. 15	174	1.6	.18	.13
12	Nov. 18	305	1.0	.31	.07
13	Nov. 19	153	2.3	.47	.14
14	Nov. 19	no overlap	1.4	.32	.12
15	Nov. 20	416	1.6	.69	.30
16	Nov. 20	336	1.1	.49	.54
17	Nov. 21	423	1.6	.51	.24
Average			1.8	.42	.28

*Not included in average.

Table 5
Summary of GRARR Data

Run No.	Date	Range RMS (meters)	Range Bias (meters)	Range Rate RMS (cm/sec)	Range Time Difference (milliseconds)
4	Aug. 10	12.9	-5.6 ± 1.0	No $\dot{R}$ data used	-1.40 ± .77
8	Oct. 6	6.4	8.7 ± 1.3	21.6	-3.75 ± .52
9	Oct. 7	6.5	10.6 ± .8	5.4	-3.28 ± .23
10	Oct. 8	6.1	-3.6 ± .8	3.3	-4.04 ± .28
11	Nov. 15	5.6	-4.1 ± 2.2	3.3	-1.73 ± 1.27
12	Nov. 18	6.1	-35.2 ± 1.0	8.6	-.82 ± .42
13	Nov. 19	5.7	-4.7 ± 1.5	9.9	-.77 ± .11
15	Nov. 20	6.2	-2.6 ± .6	2.0	-1.47 ± .17
16	Nov. 20	6.2	-10.1 ± 1.1	5.8	-2.02 ± .44
17	Nov. 21	6.2	-6.5 ± .7	2.4	-1.41 ± .17
Average		6.8	-5.3 ± 12.4	6.9	-2.07 ± 1.19

Range and range rate data is reported only for Laser passes considered acceptable. GRARR runs were made for all Laser passes where data was available; however, as expected, results were poor where Laser or GRARR malfunctions were reported.

It was felt that the standard deviation from GDAP associated with the bias figures given in Table 5 do not represent the true standard deviation that can be expected on any one pass using GRARR data with Laser defined orbits. Omitting the runs (8, 9, 12) with a bias which deviate greatly from the norm, a new average bias was calculated for the remaining seven passes. Coincidentally the new bias was calculated to be -5.3 meters.

Using the formula:

$$\sigma = \pm \sqrt{\frac{\sum_{i=1}^{N} (B_i - \overline{B})^2}{N - 1}}$$

where N = 7, $\bar{B}$ = -5.3 meters and B_i is the bias for the i$\frac{th}{}$ pass. A more realistic standard deviation of ± 2.5 meters was calculated and will be reported as the per pass standard deviation of the range bias.

Table 6
Selected Data Set Averages

	Range RMS (meters)	Range Bias (meters)	Range Rate RMS (cm/sec)	Range Time Difference (milliseconds)
Average	6.2	-4.2 ± 2.0	2.6	-2.31 ± 1.50

When the adjustment program converged for a given pass, the range and range rate residuals obtained using the final parameter set were punched out on data cards. Since range rate refraction correction was not made in the GDAP at the time of these reductions, this set of range residuals was refraction corrected and a new set of range rate residuals obtained. The final refraction corrected range and range rate residuals was input to a sequential least squares regression analysis program which was used to determine the statistical feasibility of a proposed range or range rate error model.

LASER ERRORS

For the three Laser passes used for GRARR error modeling, the Laser range residuals had a mean value of -0.002 meters and a standard deviation of 1.5 meters. A Chi-square test of normality was run on the range residuals and none of the three sets were found to be significantly non-normal, although a slight skewness was noticed in each of the three data sets. However, the residuals appeared to be random and if any systematic effects were present, they were quite small.

Tests have been made for serial correlation in the Laser data.[7,8] The results showed the serial correlation to be insignificant. Using the assumption of independence, the eigenvalues of the covariance matrix[9] of the velocity parameters $\dot{X}$, $\dot{Y}$ and $\dot{Z}$ can be used to get an estimate of the accuracy with which range rate can be determined using orbits defined by the Laser. It was calculated that range rate would be no more accurate than one centimeter per second using the Laser as a standard.

TEMPERATURE AND S/N VARIATION OF GRARR TRANSPONDER DELAY

Temperature and S/N variables in transponder delay were measured before its installation in the satellite. Table 7 summarizes these errors which may be removed by a look-up table as a function of temperature and up-link signal strength. These errors have not been removed from the data presented in this document.

Table 7
Transponder Variations with Temperature and Signal Level

Run No.	Date	Temperature (degrees centigrade)	Power Up-link 1500/3000 km	Range Variation (meters)
4	Aug. 10	4.4	-59/ -65 dbm	+ .75
8	Oct. 6	16.7	-59/ -65 dbm	+ .45
9	Oct. 7	3.6	-59/ -65 dbm	+ .78
10	Oct. 8	4.2	-59/ -65 dbm	+ .75
11	Nov. 15	-4.6	-59/ -65 dbm	+ .88
12	Nov. 18	5.1	-59/ -65 dbm	+ .73
13	Nov. 19	-8.4	-59/ -65 dbm	+1.00
15	Nov. 20	-7.9	-59/ -65 dbm	+ .98
16	Nov. 20	4.9	-59/ -65 dbm	+ .74
17	Nov. 21	-6.1	-59/ -65 dbm	+ .95

Test specifications require that the maximum tolerance for transponder delay shall not exceed 32 nanoseconds or 4.8 meters over a signal level of -15 dbm to -85 dbm with the temperature between -10° C and $\pm 45^{\circ}$ C.[10]

GRARR ANTENNA POSITION BIAS

The Rosman S-band GRARR parabolic antennas are mounted on an X-Y system. The X axis is oriented North-South and is fixed in position. The Y axis is oriented East-West, but is mounted 1.17 meters above the X axis. This causes the position of the Y axis to vary sinusoidally in respect to the geodetic location of the site. The correction in meters is:

$$\Delta R = 1.17 (\text{Cos } Y), \text{ where } Y \text{ is the } Y \text{ angle of the pedestal.}$$

ROSMAN ZERO SET BIAS

The average zero set bias for these tests after removal of known biases was -5.3 meters with a standard error of the bias estimate at 2.5 meters. Known biases, which were removed, include the 14-foot RE-142 cable used in precalibration adjustments (at the collimation tower) which accounts for 6.3 meters. Also, the displacement of the horn aperture on the collimation tower reflector, considering reflections within the cassegrainian feed system, is 1.0 meter greater than that previously used. The delay in the collimation tower transponder, when zero setting the system, has been found to be 3.0 meters greater than had been thought with respect to the test set used to calibrate both the collimation tower transponder and the satellite transponder. The 156 meters distance between the collimation tower and the tracking system antenna was measured to the stationary center of the X-axis of the GRARR antenna. The correction described in the preceding paragraph now accounts for the offset between the Y- and the X-axes, treating the data as if it were initially referenced to the center of the Y-axis and correcting it to the center of the X-axis. Therefore, the collimation tower data must be treated as if it were initially referenced to the center of the Y-axis. This requires an adjustment of 0.70 meters. These errors in the GRARR system at Rosman, North Carolina are listed in Table 8.

Table 8
GRARR System Ranging Errors for Rosman, North Carolina

Name	Range Error (meters)
Zero set bias to X-axis (already corrected at Rosman prior to transmission)	156.00
Aperture of transponder horn	-1.05
Cabling delays from aperture to transponder	-6.30
Pole beacon transponder delay	-3.00
Boresight calibration conversion, X to Y axis	+0.70
Boresight parallax error due to dish separation	-0.02
Total uncorrected error	-9.67

The net 9.7 meters correction was made in the GRARR preprocessing program.

TIMING ERRORS

The average range timing difference between the GRARR system and the Laser was -2.1 ± 1.2 milliseconds. However, this timing error appeared to drift since the errors for the October passes varied from -3.28 milliseconds to -4.04 milliseconds with an average value of -3.7 ± 0.4 milliseconds while the errors for passes in November varied from -.77 milliseconds to -2.02 milliseconds with an average value of -1.4 ± 0.5 milliseconds. Also, using techniques of linear regression, a consistent range rate timing error of -0.2 milliseconds appeared as the coefficient of the range acceleration term in the range rate model.

Part of the timing errors can be explained by two known lag delays in the circuitry of the GRARR System. Both the range and the range rate are affected by a 0.03 millisecond delay in the GRARR start pulse. Also, a narrowband, single-tuned LC circuit filter precedes the range discrimination circuit in the ground receiver. The time delay through such a circuit may be expressed as:

$$T = \frac{Q}{2\pi f_o}$$

where Q is the quality factor of the tuned circuit (measured to be equal to 84) and f_o is the major side tone frequency (100 kc).

The delay caused by this circuit is 0.13 milliseconds, giving a total explained delay of 0.16 milliseconds. This time delay has not been removed from the timing figures given in the rest of the paper.

It should be noted that the difference between the GRARR range and the GRARR range rate timing errors seems to indicate that the timing problem was not caused by the Laser, but probably by the GRARR circuitry affecting only the range measurements.

TRANSPONDER DELAY VS. DOPPLER DELAY

The up-link receiver contains a filter which produces a phase delay according to the frequency of the input. All GRARR tracks of GEOS-A used in this experiment were taken on channel A at an input frequency of 2271.9328 megacycles. This is significant since each transponder channel has a characteristic delay curve.

In September of 1964, the Military Electronics Division of Motorola, Inc. tested the delay in the GEOS-A transponder and found it to be 3511[11] nanoseconds at zero doppler for channel A. The transponder was tested again at Cape Kennedy, Florida in November 1965 prior to the launch of GEOS-A and the delay was found to be 3677 nanoseconds at zero doppler. When the GRARR data is received at GSFC, a correction of 3677 nanoseconds (551.6 meters) is made to the range data taken on channel A. The solid curve in Figure 1 shows a graph of the range error vs. range rate (doppler) based on the Motorola values. However, the entire curve has been vertically offset by a value of 166 nanoseconds (24.9 meters) to bring the delay at zero doppler to the 3677 nanosecond value used at Goddard. It was assumed that the shape of the transponder correction curve was not altered. A second degree polynomial was fit to the solid curve in Figure 1 to arrive at the transponder delay correction used in the GDAP preprocessor. The standard error of the fit for channel A was $\pm$ 0.2 meters over the operating region of GEOS-A which is between $\pm$ 50 kc doppler.

Inasmuch as there seemed to be some uncertainty about the transponder delay correction, the range residuals were subjected to a regression analysis using a second degree polynomial of the form:

$$\text{(a)} \qquad \Delta R = K_8 \dot{R}^2 + K_6 \dot{R}$$

Since this model is of the same form as the transponder correction, it was hoped that any error in the present correction could be resolved. The reduction in the rms value of the range residuals, however, was insignificant as shown in Figure 3.

Also, it was felt that any transponder errors affecting the range measurements would affect the range rate residuals in a manner represented by a differential form of the range curve (a) given by:

$$\Delta \dot{R} = 2K_4 \dot{R} \ddot{R} + K_2 \ddot{R}$$

where $\ddot{R}$ is range acceleration. Here it was expected that the regression coefficients K_4 and K_2 would be significantly similar to the coefficients of $\dot{R}^2$ and $\dot{R}$, respectively, in the range transponder correction (ΔR_2, page 6). Since this did not occur, a further search into the GRARR hardware characteristics was initiated.

Two oscillators are used in the GRARR ground station. One for the up-link carrier frequency used to extract doppler information, and the other for the ranging side tones which are phase modulated on the up-link carrier. Since the spacecraft transponder delay has a different effect on signals traveling with group velocity, such as the ranging side tones, and signals with phase velocity, such as the carrier[12], dissimilar delay characteristics of the range and the range rate are to be expected. The delay which affects the ranging side tones has been modeled; however, work is still in progress on the delay characteristics of the carrier through the transponder.

The offset oscillator on the spacecraft has an accuracy specification (see reference 10) of five parts in 10^6 or about 8.5 kHz at 1705 MHz. Any drift in the oscillator would alter the transponder curve given in Figure 1. This change in the transponder delay curve could cause an inaccurate transponder delay correction in the spacecraft range calculation causing what would appear to be a timing error and a bias error in the orbital fit. The range bias errors caused by a frequency offset would be quite small and well within the standard error of the range bias noted in this paper. However, an inaccurate zero setting of the transponder delay curve in Figure 1 could introduce a significiant range bias into the orbital fit. For example, the range bias of -5.3 meters given in this paper could have been caused by a zero set error of approximately 35 nanoseconds in the transponder delay curve, i.e., using, as a transponder delay correction, the solid curve in Figure 1, with a zero doppler correction of 3642 nanoseconds rather than the 3677 nanoseconds now used, the range biases for most GRARR passes would move to within one sigma of zero.

The magnitude of the center frequency offset necessary to fully explain the GRARR range timing errors noted in this report lies well outside the operating region of GEOS-A. However, it is felt that oscillator drift has had a significant affect on the range timing error figures. As an example of the errors caused by a frequency offset, consider a hypothetical shift S in the center frequency of the crystal oscillator aboard the spacecraft and assume no other change in shape of the transponder correction curve.

Let:

$$S = 25 \text{ kHz} \approx -3300 \text{ meters/sec.}$$

The transponder delay correction ΔR_T has the form:

$$\Delta R_T = a\dot{R}^2 + b\dot{R}$$

where $a = 7.18 \times 10^{-8}$, $b = 0.332 \times 10^{-3}$ and $\dot{R}$ is the measured range rate.

Introducing a frequency shift S, the transponder delay correction becomes:

$$\Delta R_s = a(\dot{R} + S)^2 + b(\dot{R} + S)$$

Expanding and regrouping the above expression, ΔR_s becomes:

$$\Delta R_s = \Delta R_T + 2aS\dot{R} + (aS^2 + bs)$$

Hence the error in the transponder delay correction introduced by a frequency shift S will be:

$$E_s = 2aS\dot{R} + (aS^2 + bS)$$

Assuming S to be constant over the duration of a short arc pass, E_s takes the form:

$$E_s = \Delta T\dot{R} + B$$

where

$$\Delta T = 2aS$$

$$B = aS^2 + bS$$

Using the values specified previously, the errors caused by neglecting the shift S would be:

$$\Delta T = -0.5 \text{ milliseconds}$$

$$B = -0.3 \text{ meters}$$

Thus a timing error of -0.5 milliseconds would occur if the transponder oscillator had shifted 25 kHz as shown by the dotted curve in Figure 1 and the total delay in the spacecraft transponder were still represented by the solid curve in Figure 1. As was stated previously, the range bias error caused by the shift is insignificant.

Another error model was postulated to explain range errors. It consisted of a term representing a servo lag error in the system and a timing error term and had the form:

$$\Delta R = K_7 \ddot{R} + K_6 \dot{R}$$

This model did not significantly reduce the RMS errors of the range residuals as shown in Figure 3.

RANGE RATE ERRORS

The average range rate RMS value for GDAP for the three passes which received concentrated analysis was 2.6 centimeters per second.

After the range rate residuals were corrected for ionospheric and tropospheric refraction effects[13], the average RMS was 3.6 cm/sec. Since the average RMS increased after refraction correction, there was some uncertainty about the accuracy of the functional form used. It was known that there existed a 5% uncertainty in the tropospheric correction and a 25% uncertainty in the ionospheric correction. However, after refraction correction, plots of the three sets of range rate residuals gave an "S" shaped curve similar to that of Figure 2. These results were essentially in agreement with those of other short arc orbital work using orbits defined by appropriately weighted SECOR, TRANET, GRARR and optical data[14] as well as with twenty-four hour long arc fits using GRARR data with optically defined orbits.

Since there were some misgivings on the refraction correction, a regression analysis was done using the model:

$$\Delta \dot{R} = K_5 C_R + K_1 \dot{R} + K_2 \ddot{R}$$

where

$$C_R = \frac{\dot{E} \cos E}{\sin^2 E}$$

where E is the elevation angle of the target and $\dot{E}$ is its elevation rate.

The $\dot{R}$ term, which represents a frequency error, was included since work done at D. Brown Associates (see reference 14) indicated that this term was significant. The $\ddot{R}$, representing a range rate timing error, was used since a consistent -0.2 millisecond error was noted for all three passes using range rate error model (1) in Figure 3.

The refraction parameter K_5 which was to be determined was of the form:

$$K_5 = \int_0^{\infty} N dh$$

where N was the total refractivity.

The results of the regression analysis for the refraction error model coefficient, K_5, showed a high correlation of 0.89 between the range rate residuals and C_R, indicating this term can fit the data and reduce the residuals. However, the values of K_5 were unrealistic in a physical sense and therefore it was concluded that it was better to apply the theoretical refraction correction.

The results for the $\dot{R}$ term, K_1, similarly indicated a high correlation of -.92 between the range rate residuals and the range rate. Also, the use of a model of the form:

$$\Delta \dot{R} = K_1 \dot{R}$$

reduced the average range rate residual RMS from 3.63 cm/sec to 1.36 cm/sec. In the physical GRARR system the coefficient K_1 can be derived as follows:

Using

(a) $$\dot{R} = -\frac{C f_D}{2 f_T}$$

where f_D is twice the doppler frequency and f_T is the up-link transmitter frequency.

The representation of $\dot{R}$ shown above is an approximation sufficient to determine first order effects such as transmitter frequency offset.

Differentiating (a) we get:

$$\Delta \dot{R} = -\frac{1}{2} \frac{f_D}{f_T} \Delta C + \frac{C}{2} \frac{f_D}{f_T^2} \Delta f_T$$

(b) $$\Delta \dot{R} = \left(\frac{\Delta C}{C} - \frac{\Delta f_T}{f_T}\right)\left(-\frac{C f_D}{2 f_T}\right)$$

but substituting (a) into (b)

$$\Delta \dot{R} = \left(\frac{\Delta C}{C} - \frac{\Delta f_T}{f_T}\right)\dot{R}$$

hence:

$$K_1 = \frac{\Delta C}{C} - \frac{\Delta f_T}{f_T}$$

Since the same value of C, the speed of light, is used in both the Laser and the GRARR preprocessing, any error therein would cancel. Therefore K_1 would represent an error in the transmitter frequency. The carrier frequency error obtained from K_1 was approximately 1 part in 10^5 or 22.7 kc at a frequency of 2271.9328 Mc. The ground station oscillator which produces the carrier frequency has an accuracy specification of 5 parts in 10^7 or approximately 1.1 kc for thirty days. However, drifts of as much as 4.8 kc have been noted when the thirty day calibration has been performed. Therefore, it was concluded that if there were an error in the transmitter frequency or in its value used for preprocessing, it could not be of the magnitude suggested by K_1 and hence, other systematic effects must be present. Therefore, other error models for range rate were postulated.

Since the curve in Figure 2 can be represented by many functional forms, obtaining a satisfactory error model for range rate became a matter of trial and error. Reduction in the residual RMS, consistency of error model coefficients for the three passes and physical significance were the primary prerequisites for accepting an error model term. Since a -0.2 millisecond timing error appeared consistently in all previous error models using $\ddot{R}$, this term was used with a term representing a Type II servo lag.

The model was of the form:

(a) $$\Delta \dot{R} = K_3 \dddot{R} + K_2 \ddot{R}$$

where K_2 represents the timing error and K_3 the servo lag error.

The reduction in the average RMS for the three passes was from 3.63 cm/sec to 1.84 cm/sec and, again, a timing error of -0.2 milliseconds was observed. Since the reduction in RMS was not as good as was desired and the servo lag coefficient was inconsistent, an $\dot{R}\ddot{R}$ term was added to the model (a) in order to give it the form of the differential of the transponder range delay curve, which had been tested previously, coupled with a servo lag term.

$$\Delta \dot{R} = K_3 \dddot{R} + K_2 \ddot{R} + K_4 \dot{R} \ddot{R}$$

where $K_3 \dddot{R}$ is the servo lag model and $K_2 \ddot{R} + K_4 \dot{R} \ddot{R}$ is the differential form of the transponder range delay curve. The $\dot{R} \ddot{R}$ term was retained because of its significant contribution to the reduction of the $\dot{R}$ RMS. Its physical significance in terms of the range rate delay through the transponder has not yet been determined.

The reduction of RMS from 3.63 cm/sec to 1.25 cm/sec was somewhat better than the previous model. However, it was noted theat the servo lag was the least significant term in the regression and reduced the RMS only .01 cm/sec. Therefore, a servo lag error was eliminated from further consideration in the range rate error modeling.

The final range rate error model consisted of all terms which appeared significant in the previous models tested and was of the form:

$$\Delta \dot{R} = K_5 C_R + K_1 \dot{R} + K_2 \ddot{R} + K_4 \dot{R} \ddot{R}$$

Using this model, a significant reduction in average RMS from 3.63 cm/sec to 1.01 cm/sec was observed.

As previously stated, using the Laser orbits as a standard, the accuracy of range rate could be determined to no better than 1 cm/sec. Therefore, this model seemed to define the range rate errors as well as could be expected.

The most significant term in the regression was the $\dot{R} \ddot{R}$ term followed by the $\ddot{R}$ term, while the $\dot{R}$ and refraction (C_R) terms appeared to be of equal significance. That is, when either the $\dot{R}$ term of the C_R term was entered into the regression, the addition of the other term did not affect the fit at all. Therefore, both the model

$$\Delta \dot{R} = K_5 C_R + K_2 \ddot{R} + K_4 \dot{R} \ddot{R}$$

and the model

$$\Delta \dot{R} = K_1 \dot{R} + K_2 \ddot{R} + K_4 \dot{R} \ddot{R}$$

explained the range rate residual curve of Figure 2 to the expected accuracy. The coefficients K_2 and K_4 showed consistency, whereas the coefficients of C_R and $\dot{R}$ did not. This makes it difficult to justify their presence in the error model, though the presence of one or the other contributed to a reduction in the RMS value.

ANTENNA MOTION DOPPLER

A further correction to the range rate values due to motion of the antenna about the X-axis is suggested and will be implemented in further analysis done on the GRARR system. It was felt that the range rate accuracy attainable in this experiment did not warrant its inclusion; however, in work where better accuracy is required it will be added. The correction should be added to the range rate measurement and is given in meters per second by:

$$\Delta \dot{R} = -1.17\dot{Y} \sin Y$$

where Y is the Y angle of the GRARR antenna and Y is its rate of change. For GEOS-A the maximum value of the correction is about 0.2 cm/sec.

ERROR IN PROPAGATION ANOMALY

A tropospheric correction only is made to the range measurements in the GDAP. The functional form to be added to the range is given by:

$$\Delta R_T = \frac{-2\alpha}{\sin E + \sqrt{\sin^2 E + \frac{4H_T}{r_o}}}$$

where H_T is the scale height of the troposphere, r_o is the earth radius, E is the elevation angle of the spacecraft and

$$\alpha = (n_o - 1)\left[(n_o - 1)\ r_o + H_T\right]$$

where n_o is the ground index of refraction. The nominal tropospheric zenith correction for range is approximately -2.0 ± 0.1 meters.

The range rate residuals are corrected for tropospheric and ionospheric refraction after being processed by GDAP. The index of refraction n_o used for the tropospheric refraction correction is calculated using the pressure, temperature and humidity at the station at the time of the pass. As was stated previously, this correction is known to be in error by as much as 5%. The ionospheric portion of the correction is known to be in error by as much as 25%.

The functional form for the total range rate refraction correction to be added to the range rate is given by:[13]

$$\Delta \dot{R} = \frac{\dot{E}\cos E}{\sin^2 E}\left[\left(\int_0^\infty N_i dh + \frac{n_o}{k}\right) + \frac{1 - \frac{3}{\sin^2 E}}{r_o}\left(\int_0^\infty N_i h dh + \frac{n_o}{k^2}\right)\right]$$

where N_i is the ionospheric refractivity and $\dot{E}$ the elevation rate of the spacecraft. The terms containing n_o and k give the tropospheric portion of the refraction correction, k is a table look-up function of n_o.[15]

A similar form[13] due to J.J. Freeman for the range ionospheric refraction correction is given by:

$$\Delta R = \frac{1}{\sin E}\left[\int_0^\infty N_i dh - \frac{\cot^2 E}{r_o} \int_0^\infty N_i h dh\right]$$

The nominal ionospheric range refraction at zenith for passes at night is 0.5 ± 0.13 meters.

There was some uncertainty about the refraction corrections used since the up-link carrier frequency of 2271.9328 mc from which doppler is derived is retransmitted down-link with a frequency of 1705 mc. The fact that the up-link carrier effectively traveling with phase velocity and the down-link subcarrier traveling with group velocity are at different frequencies had not been taken into account in the refraction correction. In order to remedy this situation in the future, equivalent frequencies for both range and range rate refraction corrections will be used rather than the up-link frequency now used. These frequencies are derived as follows.

Both $\int_0^\infty N_i dh$ and $\int_0^\infty N_i h dh$ are functions of the maximum usable frequency at 3000 km (MUF (3000)), the plasma frequency, f_o, and the operating frequency of the system, f.[15] The values of MUF (3000) and f_o for a given month at a given position can be obtained from the CRPL Ionospheric Prediction Map. Hence, given the month and the position of the tracking system:

$$\int_o^\infty N_i dh = A\left(\frac{1}{f^2}\right) \quad \text{and} \quad \int_o^\infty N_i h dh = B\left(\frac{1}{f^2}\right)$$

where A and B are constant

Therefore, given the radius of the earth, r_o, both the range and the range rate refraction corrections at a given elevation will be inversely proportional to the operating frequency squared.

Since the ranging sidetones travel with group velocity both up-link and down-link it is sufficient to average the up-link (ΔR_U) and down-link (ΔR_D) refraction corrections to get the equivalent refraction correction (ΔR_{eq}) for range. Therefore

$$\Delta R_{eq} = \frac{1}{2} (\Delta R_U + \Delta R_D)$$

Using the up-link (f_U) and down-link (f_D) frequencies it is possible to calculate a single equivalent frequency (f_{eq}) to be used in the standard refraction correction model.

Since for a given elevation and under given environmental conditions the refraction correction is inversely proportional to the operating frequency squared:

$$\frac{1}{f_{eq}^2} = \frac{1}{2}\left[\left(\frac{1}{f_U^2}\right) + \left(\frac{1}{f_D^2}\right)\right]$$

(a) $$f_{eq} = f_U f_D \sqrt{\frac{2}{f_D^2 + f_U^2}}$$

For channel A, $f_U = 2272$ Mc and $f_D = 1705$ Mc

Substituting in (a)

$$f_{eq} \text{ (range)} = 1928 \text{ Mc}$$

For GEOS-A at an elevation of 30 degrees the range refraction correction using the equivalent frequency would be approximately 0.3 meters greater than that using the GRARR up-link frequency.

For range rate the derivation is similar however it is necessary to reverse the sign of the index of refraction used in the up-link refraction correction since the carrier travels with phase velocity up-link.[16] Thus:

$$\Delta \dot{R}_{EQ} = \frac{1}{2}\left(\Delta \dot{R}_D - \Delta \dot{R}_U\right)$$

As in the range calculation:

$$\frac{1}{f_{eq}^2} = \frac{1}{2}\left[\left(\frac{1}{f_D^2}\right) - \left(\frac{1}{f_U^2}\right)\right]$$

(b) $$f_{eq} = f_U f_D \sqrt{\frac{2}{f_U^2 - f_D^2}}$$

Substituting in (b)

$$f_{eq} \text{ (range rate)} = 3648 \text{ Mc}$$

For GEOS-A at an elevation of 30 degrees the range rate refraction correction using the equivalent frequency would be approximately 0.1 cm/sec less than that using the GRARR up-link frequency.

RANGE RATE AVERAGING ERROR

This correction was not used in the intercomparison investigation but will be used in further processing of range rate data. This error[17] is due to approximating the instantaneous value of range rate by the average value over an interval ΔT. For an orbit such as that of GEOS-A a maximum error of about 0.7 cm/sec could occur in the range rate. The correction is added to the measured range rate and is given by:

$$\Delta \dot{R} = -\frac{\dddot{R}\,(\Delta T)^2}{24}$$

where $\dddot{R}$ is the third time derivative of range.

CONCLUSIONS AND SUMMARY

The GRARR range bias of -5.3 $\pm$ 2.5 meters and the range timing error of -2.1 $\pm$ 1.2 milliseconds could be explained in part by inaccuracies in the transponder delay curve. More passes must be analyzed to determine the magnitude of this effect.

A consistent range rate timing error of -0.20 $\pm$ .02 milliseconds was observed, but its cause has not been detected. The "S" shaped range rate residual curve observed in both short arc and long arc orbital work can be satisfactorily defined to 1 cm/sec RMS by the model:

$$\Delta\dot{R} = K_1\dot{R} + K_2\ddot{R} + K_4\dot{R}\ddot{R}$$

This curve and, hence, the above model may be altered by further refinements in the range rate refraction correction.

From this intercomparison experiment it appears that Laser orbits can be used to detect systematic errors in both the range and the range rate to about 2 meters and 1 cm/sec respectively. After editing the Laser data, systematic effects therein seemed to be at a minimum.

It is felt from the work done here that for future spacecrafts carrying transponders, if a more thorough analysis is made of the delay and draft characteristics of the transponder, the GRARR system accuracy may exceed the 15 meter and 10 cm/sec design goals for the range and range rate measurements. It would be helpful in determining transponder inaccuracies if the drift in the down-link frequency could be measured and recorded periodically.

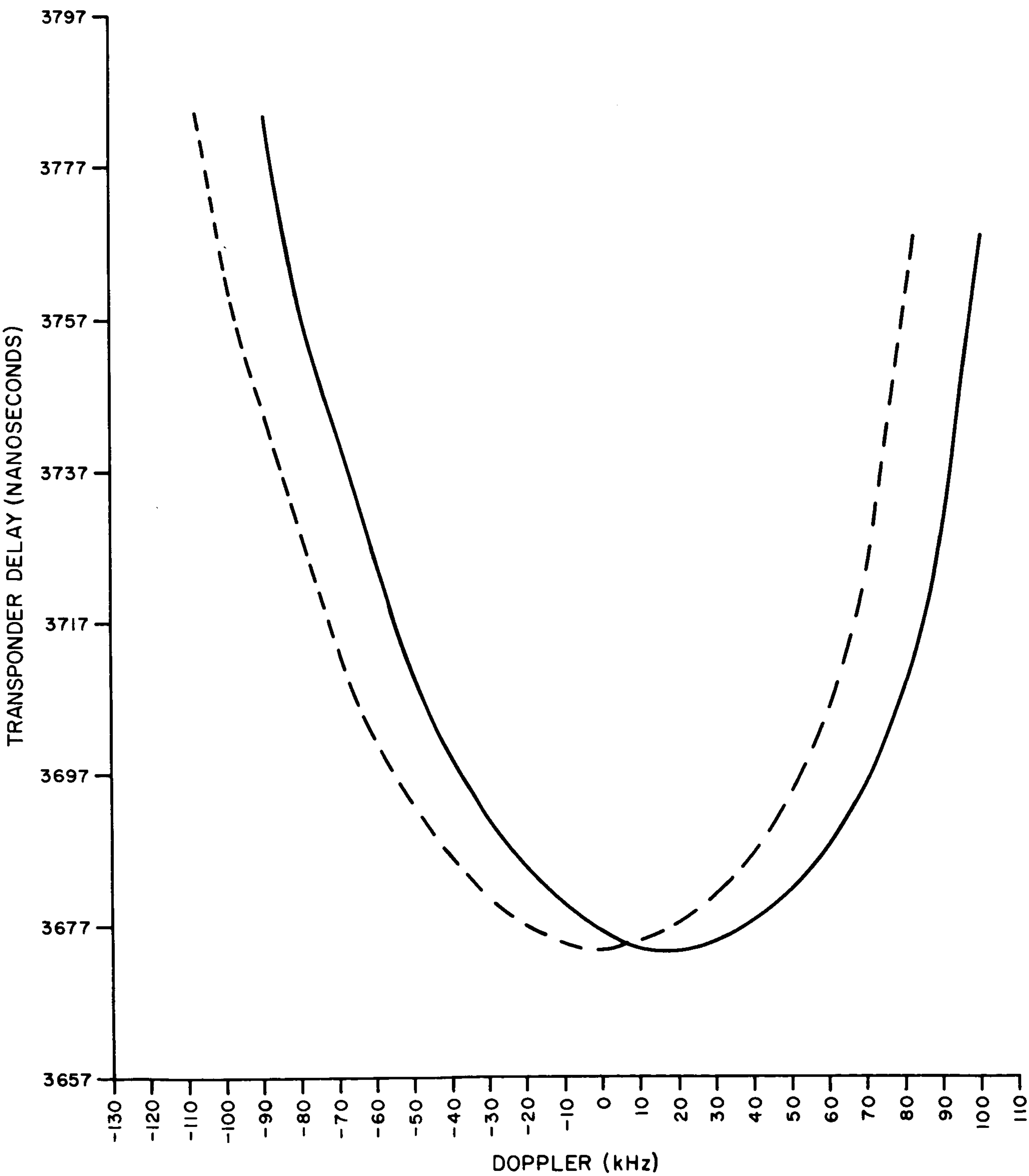

Figure 1. Range Error (Transponder Delay) vs. Doppler (Range Rate)

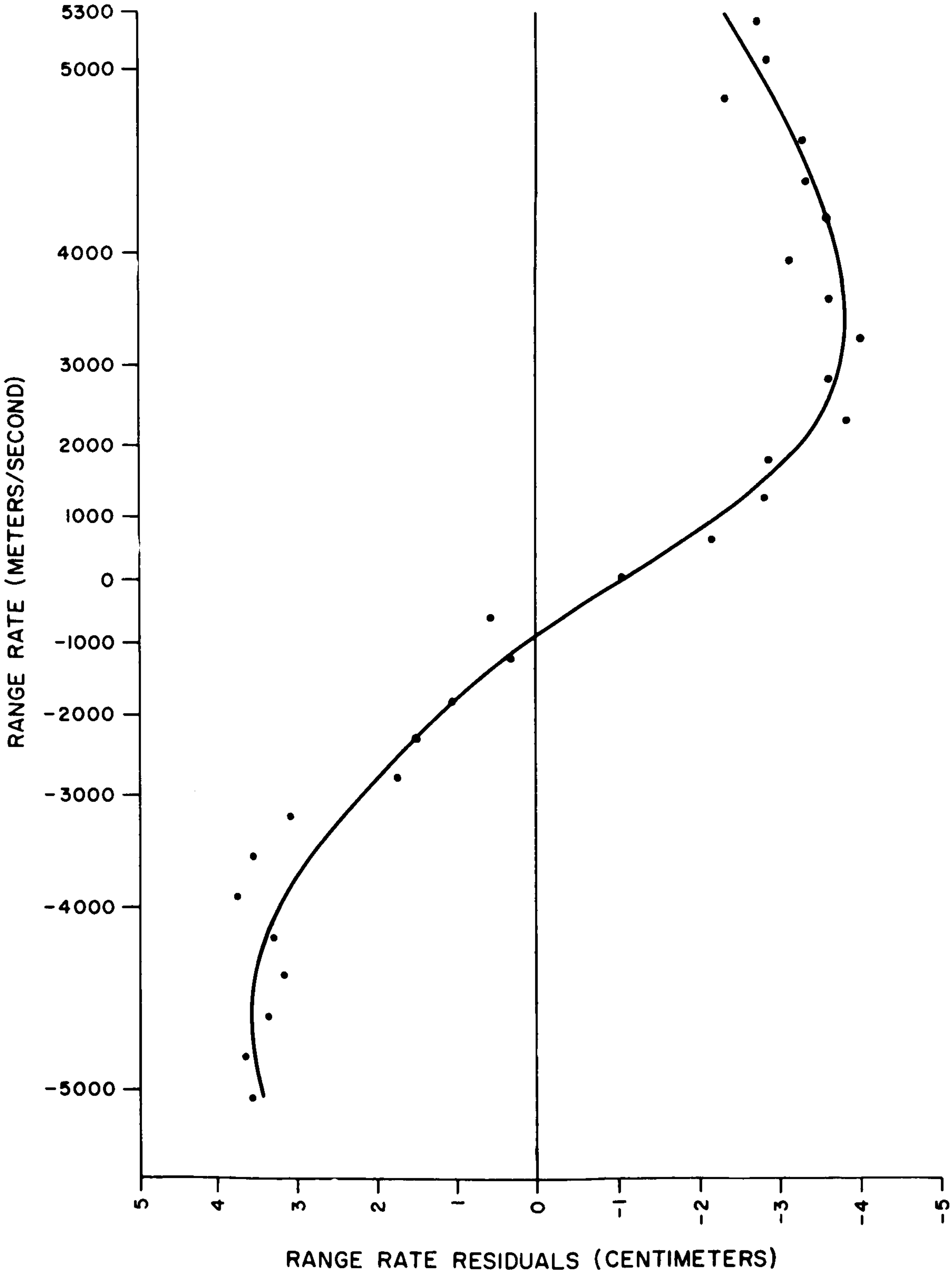

Figure 2. Range Rate Residual Curve

RANGE ERROR MODELS	
INITIAL RANGE RMS 6.2 METERS	
MODEL	FINAL RMS
(1) $\Delta R = K_8 \dot{R}^2 + K_6 \dot{R}$	6.1
(2) $\Delta R = K_7 \ddot{R} + K_6 \dot{R}$	6.1

RANGE RATE ERROR MODELS	
INITIAL RANGE RATE RMS 2.6 CM/SEC	
MODEL	FINAL RMS
(1) $\Delta \dot{R} = 2K_4 \dot{R}\,\ddot{R} + K_2 \ddot{R}$	1.26
(2) $\Delta \dot{R} = K_5 C_R + K_1 \dot{R} + K_2 \ddot{R}$	1.09
(3) $\Delta \dot{R} = K_1 \dot{R}$	1.36
(4) $\Delta \dot{R} = K_3 \dddot{R} + K_2 \ddot{R}$	1.84
(5) $\Delta \dot{R} = K_3 \dddot{R} + K_2 \ddot{R} + K_4 \dot{R}\,\ddot{R}$	1.25
(6) $\Delta \dot{R} = K_5 C_R + K_1 \dot{R} + K_2 \ddot{R} + K_4 \dot{R}\,\ddot{R}$	1.01
(7) $\Delta \dot{R} = K_1 \dot{R} + K_2 \ddot{R} + K_4 \dot{R}\,\ddot{R}$	1.01

R — Range

$\dot{R}$ — Range rate

$\ddot{R}$ — Range acceleration

$\dddot{R}$ — Range-rate acceleration

Figure 3. GRARR Error Models

Table 9
Coefficients of GRARR Error Models

Range Rate Error Model No.	Range Rate Coefficients*					Range Error Model No.	Range Coefficients*		
	K_1	K_2	K_3	K_4	K_5		K_6	K_7	K_8
1		$-.20 \pm .01$		$-.51 \times 10^{-6} \pm .6 \times 10^{-8}$		1	Insignificant		$-.4 \times 10^{-7} \pm .1 \times 10^{-7}$
2	-24 ± 1	$-.16 \pm .02$			$-3.6 \pm .3$	2	Insignificant	$.14 \pm .10$	
3	-10 ± 3								
4		$-.20 \pm .02$	$.45 \pm .10$						
5		$-.21 \pm .01$	$.17 \pm .10$	$-.58 \times 10^{-6} \pm .2 \times 10^{-8}$					
6	-11 ± 2	$-.21 \pm .01$		$-.33 \times 10^{-6} \pm 2.6 \times 10^{-8}$	$-.7 \pm .5$				
7	-15 ± 1	$-.20 \pm .01$		$-.47 \times 10^{-6} \pm 1.1 \times 10^{-8}$					

* K_1 = transmitter frequency error (in parts/million)
K_2 = range rate timing error (in milliseconds)
K_3 = range rate servo lag error (in seconds)
K_4 = transponder delay term (in seconds^2/meter)
K_5 = range rate refraction error (in centimeters/second)
K_6 = range timing error (in milliseconds)
K_7 = range servo lag error (in seconds)
K_8 = transponder delay term (in seconds^2/meter)

REFERENCE LIST

1. D. Brown Associates, "Geodetic Data Analysis For GEOS A, An Experimental Design." NASA Contract NAS 5-9860, Final Report.

2. Ralston and Wilf, "Mathematical Methods for Digital Computers," Published by John Wiley & Sons, Inc., 1960.

3. IBM Share Library Program SDA 3145, "Stepwise Multiple Regression with Variable Transformations," M. A. Efroymson.

4. "Goddard Range and Range Rate System Design Evaluation Report," NASA Contract NAS 5-1926.

5. Kronmiller, G. C., Jr., and Baghdady, E. J., "The Goddard Range and Range Rate Tracking System: Concept, Design and Performance," GSFC Document X-531-65-403, October 1965.

6. Berbert, J. H., Reich, R., Stephenson, J., "Evaluation of Range Accuracy for the Goddard Range & Range Rate System at Rosman," GSFC Document X-514-66-513, October 1966

7. Wells, W. T., Moss, S. J.,"A Study of Some of the Statistical Properties of Measurements from the Goddard Laser Tracking System," NASA Contract NAS 5-9756-37, October 20, 1966.

8. Moss, S. J., Wells, W. T., "An Analysis of GSFC Laser Range Data," NASA Contract NAS 5-9756-58, May 18, 1967.

9. U.S.A.F. Space Track Center - Control Division, "Capabilities and Limitations of Field Reduced Baker-Nunn Reference Orbits," Operating Memo No. 13, May 25, 1965.

10. Motorola, Inc., Military Electronics Division, "Handbook - Goddard Range and Range Rate System," Vol. I, (Part 1), NASA Contract NAS 5-1926.

11. Motorola, Inc., Military Electronics Division, "Final Test Data for Goddard RARR Transponder," NASA Contract NAS 5-3854.

12. King, R. W. P., "Transmission Line Theory," Published by McGraw-Hill Book Co., Inc., 1955.

13. J. J. Freeman Associates Inc., "Final Report on Ionospheric Correction to Tracking Parameters," NASA Contract NAS 5-9782.

14. Berbert, J. H., "Intercomparison of GEOS-A Observation Systems," GSFC Document X-514-67-315, July 1967.

15. B.R. Bean and G.D. Thayer, "CRPL Exponential Reference Atmosphere."

16. Berkowitz; R.S., "Modern Radar Analysis, Evaluation and System Design", P351-352, Published by John Wiley & Sons, Inc., 1965.

17. Kruger, B., "The Range Rate Error Due to The Averaging Techniques of Doppler Measurements", GSFC Document X-513-65-100, March 5, 1965.